ARTICLE

OBC
www.rsc.org/obc

Absolute configuration and predominant conformations of 1,1-dimethyl-2-phenylethyl phenyl sulfoxide†

Ana G. Petrovic,[a] Jiangtao He,[a] Prasad L. Polavarapu,*[a] Ling S. Xiao[b] and Daniel W. Armstrong[b]

[a] *Department of Chemistry, Vanderbilt University, Nashville, TN, 37235, USA. E-mail: Prasad.L.Polavarapu@vanderbilt.edu*

[b] *Department of Chemistry Iowa State University, Ames, Iowa, 50011, USA*

Received 25th January 2005, Accepted 30th March 2005
First published as an Advance Article on the web 20th April 2005

The absolute configuration of the (+)-1,1-dimethyl-2-phenylethyl phenyl sulfoxide is determined to be (*R*), using three different chiroptical spectroscopic methods, namely vibrational circular dichroism (VCD), electronic circular dichroism (ECD) and specific rotation. Four solution conformations are identified for 1,1-dimethyl-2-phenylethyl phenyl sulfoxide. In each of the methods used, experimental data for the enantiomers of 1,1-dimethyl-2-phenylethyl phenyl sulfoxide were measured in the solution phase and concomitant quantum mechanical calculations of corresponding properties were carried out using density functional theory with B3LYP functional and 6-31G* and 6-31+G basis sets. Additional VCD and ECD calculations were also undertaken with 6-311G(2d,2p) basis set. A comparison of theoretically predicted data with the corresponding experimental data has allowed us to elucidate the absolute configuration and predominant conformations of (+)-1,1-dimethyl-2-phenylethyl phenyl sulfoxide.

Introduction

Chiral sulfoxides[1] are of considerable importance as bioactive compounds and synthetic intermediates. These molecules are often used as ligands for stereoselective and asymmetric syntheses. There are numerous examples in which chiral sulfoxides played a major role in preparing a final chiral product. Satoh and Kuramochi have reported the synthesis of chiral allenes by first coupling alkenyl aryl sulfoxides with aldehydes, followed by alkyl anion induced elimination of the sulfur.[2] Toru and coworkers have reported the enantioselective addition of Grignard reagents to 1-(arylsulfinyl)-2-naphthaldehyde, where a chiral sulfoxide conformer controls stereoselectivity of the addition.[3] The same group has reported[4] the use of a chiral sulfoxide to synthesize an insecticidal chiral chrysanthamate. Ellman and coworkers[5] and Yuste, *et al.*[6] have independently described the use of sulfoxides in asymmetric synthesis of β-amino alcohols, which, in turn, are synthetically useful chiral building blocks. Colobert *et al.*[7] and Bravo *et al.*[8] have demonstrated the use of chiral sulfoxides in the synthesis of myo-inositol, pyrrolidine and tetrahydroisoquinoline alkaloids. Over the years, chiral sulfoxides have clearly demonstrated wide versatility as chiral auxiliaries in stereoselective and asymmetric synthesis.

Nevertheless, prior to the application of a chiral sulfoxide as a ligand which facilitates stereospecificity for the synthetic product, it is important to determine its absolute configuration and conformation. Although X-ray crystallography is a widely used approach for this purpose, suitable quality crystals are required which may not be possible in many cases. Nevertheless for some liquid sulfoxide samples, complexes prepared with a suitable substrate could be grown into single crystals and studied.[9] Another possible approach for chiral sulfoxides[10] is the utilization of NMR with a suitable chiral shift regent. In recent years, the three chiroptical spectroscopic techniques that became popular for accomplishing configurational and conformational assignments are vibrational circular dichroism (VCD),[11] optical rotation (OR)[12] and electronic circular dichroism (ECD).[13] These three techniques are becoming increasingly useful approaches for determining the absolute configuration of chiral compounds due to the availability of quantum mechanical methods that are necessary to predict these properties reliably.[11,12,14] A comparison between predicted and observed chiroptical spectroscopic properties allows the determination of absolute configuration. Although empirical correlations between ECD and structures of sulfoxides have been available for some time,[15a] and a few coupled-oscillator calculations of ECD have been reported,[15b,c] surprisingly calculations of ECD with density functional theory (DFT) have not been reported for chiral sulfoxides. A few chiral sulfoxides have been investigated before using VCD[9b,15d–h] and optical rotation.[15i] But the absolute configuration or predominant conformations of 1,1-dimethyl-2-phenylethyl phenyl sulfoxide, **1**, (Fig. 1) have not been determined before using spectroscopic methods. The current study utilizes a combination of VCD, optical rotation and ECD by comparing the experimental measurements with corresponding quantum mechanical predictions to determine the absolute configuration and predominant conformations of **1**.

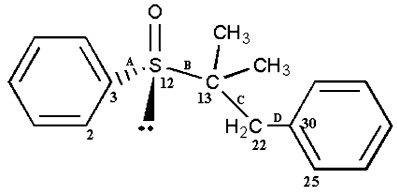

Fig. 1 The chemical structure of (*R*)-1,1-dimethyl-2-phenylethyl phenyl sulfoxide. The atom numbers shown are used to define the dihedral angles.

Results and discussion

A consideration of the rotation around four bonds (labeled as A, B, C and D in Fig. 1), indicating four dihedral angles that can be varied, suggests $3^4 = 81$ possible conformations for **1**. Each of the four dihedral angles can be rotated in increments of 120° giving: plus *gauche*, minus *gauche*, and *anti* conformations around each of the four bonds. The rotation around bonds labeled as B and C, which involves varying dihedral angles D(3,12,13,22) and D(12,13,22,30), respectively (Fig. 1), is considered first. The three conformations obtained by the variation of each

† Electronic supplementary information (ESI) available: Dihedral angles, energies, vibrational absorption, VCD and ECD spectra of four low energy conformers optimized with B3LYP/6-31+G and B3LYP/6-311G(2d,2p) basis sets (Tables S1–S2, Figs. S1–S6). See http://www.rsc.org/suppdata/ob/b5/b501220a/

DOI: 10.1039/b501220a

of these dihedral angles are labeled as T, G^+ and G^- (Fig. 2) depending on the relative orientation of the two largest end-groups defining the dihedral angle. Combination of T, G^+ and G^- conformations associated with the two dihedral angles has resulted in nine distinct conformations, TT, TG^+, TG^-, G^+T, G^+G^+, G^+G^-, G^-T, G^-G^+, G^-G^-. The geometry optimizations of these nine conformations using B3LYP functional and 6-31G* basis set have yielded eight stable conformations and the conformation G^-G^+ has converged into G^-T. A comparison of the electronic energies of the eight sulfoxide conformers has led to the identification of four low energy conformers (G^+T, TG^+, TT and G^-T) that would have significant population. The electronic energies of these eight conformers are given in Table 1.

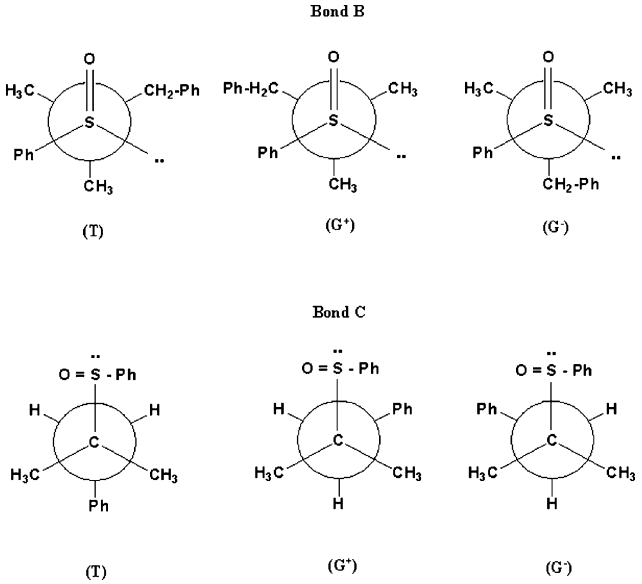

Fig. 2 Newman projections around bonds B and C for (*R*)-1,1-dimethyl-2-phenylethyl phenyl sulfoxide. For definition of bonds B and C see Fig. 1.

Table 1 B3LYP/6-31G* predictions of electronic energies for eight optimized conformers of 1,1-dimethyl-2-phenylethyl phenyl sulfoxide

Conformer[a]	Electronic energies[b]
TT	−1093.91582442
TG^+	−1093.91629803
TG^-	−1093.91088328
G^+T	−1093.91612233
G^+G^+	−1093.91103237
G^+G^-	−1093.90955477
G^-T	−1093.91534617
G^-G^-	−1093.91194699

[a] T, G^+ and G^- represent *anti*, plus *gauche* and minus *gauche* conformers. The first letter represents the conformation around bond B and the second letter around bond C. [b] in Hartrees.

The above mentioned four low energy conformers have been subjected to further geometry optimization by incrementally rotating (45° at a time) the phenyl groups at the end of bonds A and D. Since the phenyl ring is planar, four rotations (each of 45°) are sufficient. Rotations around bonds A and D correspond to changes in dihedral angles D(2,3,12,13) and D(13,22,30,25), respectively. A comparison of the energies as a function of phenyl ring rotation indicated that the four conformations, as summarized in Table 2 and displayed in Fig. 3, are the most stable. Since the magnitudes of optimized dihedral angles D(2,3,12,13) and D(13,22,30,25) are close to 90°, the conformation around Ph–S and Ph–C bonds cannot be classified as *gauche* or *anti*.

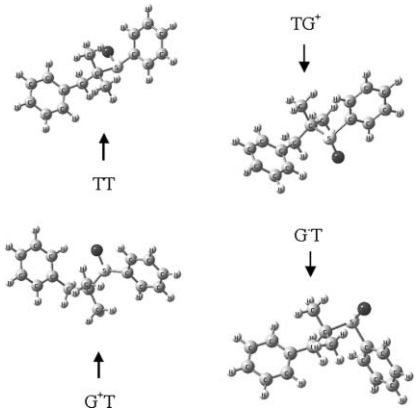

Fig. 3 B3LYP/6-31G* optimized structures for four conformers of (*R*)-1,1-dimethyl-2-phenylethyl phenyl sulfoxide.

These four conformations have been used for calculating VCD, optical rotation and ECD using the B3LYP functional and 6-31G* basis set. From the calculated vibrational frequencies, these four conformations are found to represent minima on the potential energy surface, as there are no imaginary frequencies. The theoretically predicted absorbance and VCD spectra have been obtained by scaling the absorption and VCD intensities of each of the four conformers by their corresponding populations, which are determined using the Gibbs free energies obtained in the frequency calculation. The values of converged dihedral angles discussed above as well as the populations determined from Gibbs free energies are given in Table 2.

The above mentioned four low energy conformers have also been optimized using larger 6-31+G and 6-311G(2d,2p) basis sets, both with B3LYP functional, and the results obtained are similar to those of the B3LYP/6-31G* calculation.

The calculated vibrational absorption spectra for individual conformers and population weighted predicted vibrational absorption spectrum are compared to the experimental absorption spectrum of **1** in Fig. 4. The absorption band with largest intensity at 1011 cm^{-1} in the predicted spectrum corresponds to the corresponding band in the experimental spectrum at 1047 cm^{-1}. Based on relative intensities and proximity in their positions, the

Table 2 B3LYP/6-31G* predictions of converged dihedral angles, energies and fractional populations of the four minimum-energy conformers of 1,1-dimethyl-2-phenylethyl phenyl sulfoxide

	Converged dihedral angles[b]					
Conformers[a]	D(2,3,12,13)	D(3,12,13,22)	D(12,13,22,30)	D(13,22,30,25)	Gibbs energies[c]	Fractional population
G^+T	85.2	61.3	169.4	−93.6	−1093.661842	0.47
TG^+	85.1	168.3	62.5	−91.9	−1093.661097	0.21
TT	86.0	178.1	−178.5	−90.4	−1093.660858	0.17
G^-T	87.0	−64.6	−172.0	−88.2	−1093.660744	0.15

[a] T, G^+ and G^- represent *anti*, plus *gauche* and minus *gauche* conformers. The first letter represents the conformation around bond B and the second letter around bond C. See Figs. 1–3. [b] D stands for dihedral angle in degrees. The numbers inside the parentheses indicate atom-numbers, as shown in Fig. 1. [c] in Hartrees.

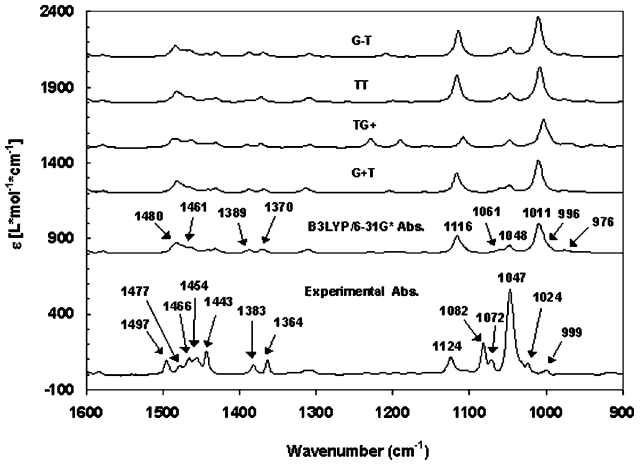

Fig. 4 B3LYP/6-31G* calculated vibrational absorption spectra for four conformers (top four traces), population weighted predicted absorption spectrum of 1,1-dimethyl-2-phenylethyl phenyl sulfoxide and experimental (bottom trace, 0.1355 M in CCl_4 solvent; path length 200 μm) absorption spectrum of 1,1-dimethyl-2-phenylethyl phenyl sulfoxide. Lorentzian band shapes and 5 cm^{-1} half-width (at half-peak height) were used in spectral simulation; 6-31G* frequencies were scaled by 0.9613.

remaining bands in the predicted spectrum at 1048, 1061, 1116, 1370, 1389 cm^{-1} and in the 1500–1450 cm^{-1} region are considered to correspond to the bands in the experimental spectrum at 1072, 1082, 1124, 1364, 1383 cm^{-1} and in the *ca.* 1500–1400 cm^{-1} region, respectively. In the predicted spectrum, relative intensities of the two bands at 1048 and 1061 cm^{-1} are interchanged and the bands in the *ca.* 1500–1400 cm^{-1} region are poorly resolved, compared to the corresponding experimental bands. The predicted vibrational band positions and corresponding experimental band positions differ by a significant amount in some cases even after scaling the calculated frequencies. Larger basis sets would be required to eliminate these differences.

The calculated VCD spectra for individual conformers and the population weighted predicted VCD spectrum for (*R*)-**1** are compared to the experimental VCD spectrum of (+)-**1** in Fig. 5. As can be seen in these spectra, only a few and weak VCD bands are seen in the experimental VCD spectrum of (+)-**1** and in the predicted spectrum of (*R*)-**1**. The only characterizing VCD signature for this molecule is a negative–positive VCD couplet seen in the experimental spectrum at 1466–1454 cm^{-1}, which is correctly reproduced in the predicted spectrum at 1480–1461 cm^{-1}.

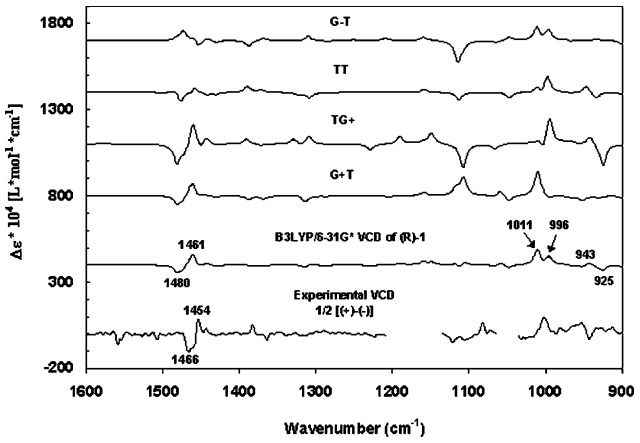

Fig. 5 B3LYP/6-31G* calculated VCD spectra for four conformers (top four traces), population weighted predicted VCD spectrum of (*R*)-1,1-dimethyl-2-phenylethyl phenyl sulfoxide and experimental (bottom trace, 0.1355 M in CCl_4 solvent; path length 200 μm) VCD spectrum of (+)-1,1-dimethyl-2-phenylethyl phenyl sulfoxide. Lorentzian band shapes and 5 cm^{-1} half-width (at half-peak height) were used in spectral simulation; 6-31G* frequencies were scaled by 0.9613.

It should be noted that the experimental VCD spectrum in two regions (1136–1211 cm^{-1} and 1066–1035 cm^{-1}) is not displayed. The first region has been eliminated due to the presence of an artefact, and the second region has been eliminated because of the interference from solvent absorption. Additionally, even after scaling the calculated frequencies by a constant, there is some mismatch in peak positions between the experimental and theoretical spectra.

Vibrational absorption and VCD calculations have also been carried out using larger 6-31+G and 6-311G(2d,2p) basis sets, both with B3LYP functional. The quality of overall comparison between predicted and experimental spectra is identical to that in the B3LYP/6-31G* calculation. Therefore B3LYP/6-31+G and B3LYP/6-311G(2d,2p) results are not displayed here, but provided as supplementary material.†

The agreement seen between predicted and experimental VCD (Fig. 5) bands suggests that the absolute configuration of **1** is (+)-(*R*) or (−)-(*S*). However, because of the limited number of weak VCD bands associated with this molecule it is prudent to verify this conclusion with other chiroptical spectroscopic methods. For this reason we have also carried out OR and ECD studies, as described below.

The experimental optical rotations and specific rotations for the first eluted enantiomer as a function of concentration are shown at 589 and 365 nm in Fig. 6. The experimental value of intrinsic rotation (specific rotation at infinite dilution) is 79 ± 4 at 589 nm and $(5.7 \pm 0.1) \times 10^2$ at 365 nm. The specific rotations were predicted with B3LYP functional and 6-31G* basis set for the four optimized conformers with (*R*)-configuration. The population weighted specific rotation obtained with 6-31G* basis set, with populations given in Table 2, are 148 at 589 nm and 858 at 365 nm. Even though the magnitudes of predicted specific rotation are *ca.* 2 times larger than those of observed intrinsic rotation, the sign of rotation predicted for (*R*)-**1** supports the absolute configuration assigned for **1** from VCD data. For a quantitative agreement between observed and predicted rotations, one has to consider the additional factors such as higher level basis sets and solvent influence. The calculations repeated with B3LYP functional and a larger 6-31+G basis set yielded the population weighted specific rotation of 123 at 589 nm and 826 at 365 nm. These values also confirm the absolute configuration as (+)-(*R*) for **1**.

The ECD spectra calculated for individual conformers of (*R*)-**1** with the B3LYP functional and 6-31G* basis set, along with the population weighted ECD spectrum, are compared to the experimental ECD spectrum of (+)-**1** in Fig. 7. In the experimental spectrum presented, ECD intensities were scaled up by a factor of 6. The positions for ECD intensity maxima in the predicted population weighted spectrum do not match those in the experimental ECD spectrum and the predicted ECD intensity magnitudes are also not in quantitative agreement with the experimental ECD intensity magnitudes. Nevertheless, the experimental ECD spectrum shows a broad positive ECD band in the long wavelength region and a negative ECD band in the shorter wavelength region. The same features are seen in the population weighted predicted spectrum, again confirming the (+)-(*R*)-**1** assignment derived from VCD and OR data. As an additional verification, ECD spectra for (*R*)-**1** were also predicted with B3LYP functional and two larger basis sets, 6-31+G and 6-311G(2d,2p), and the results obtained in these calculation (not shown, but provided as supplementary material)† are found to be similar to those in the above discussed B3LYP/6-31G* calculation.

Conclusions

The following conclusions are derived from a combined study of VCD spectra, optical rotation and ECD spectra. (1). The predominant conformations of 1,1-dimethyl-2-phenylethyl phenyl sulfoxide molecule are the conformations labelled as G^+T,

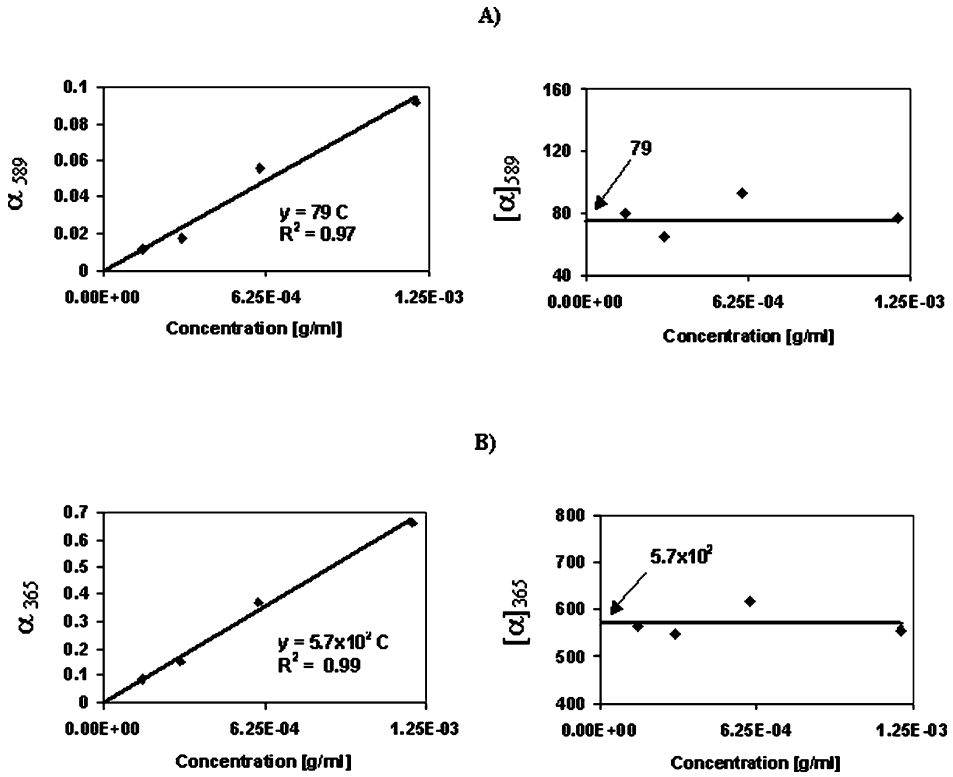

Fig. 6 The experimental (room temperature) optical rotation (left panels), a, and specific rotation (right panels), $[a]$, of (+)-1,1-dimethyl-2-phenylethyl phenyl sulfoxide as a function of concentration (C, in g cm^{-1}) at 589 nm (top panels) and 365 nm (bottom panels). The observed rotations were fit to a linear equation (listed on the left panels). The experimental specific rotation values are: $[a]_{589} = 79\ (\pm 4)$ and $[a]_{365} = 5.7\ (\pm 0.1) \times 10^2$.

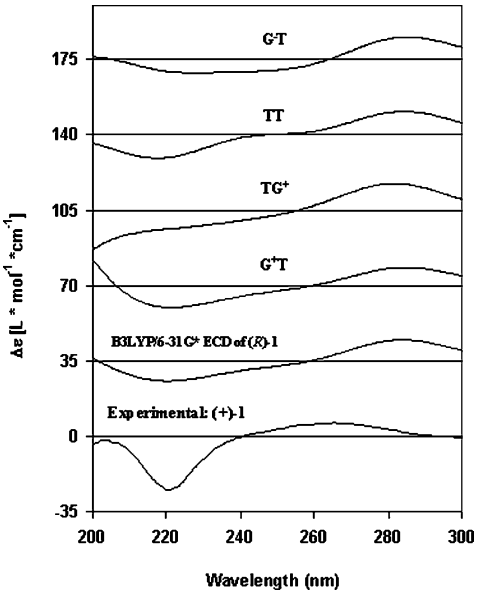

Fig. 7 B3LYP/6-31G* calculated ECD spectra for four conformers (top four traces), population weighted predicted ECD spectrum of (*R*)-1,1-dimethyl-2-phenylethyl phenyl sulfoxide and experimental (bottom trace) ECD spectrum of (+)-1,1-dimethyl-2-phenylethyl phenyl sulfoxide. The experimental ECD intensities presented in this figure were scaled up by a factor of six. Gaussian band shapes and 20 nm half-width (at 1/e of peak height) were used to simulate the predicted spectra.

TG$^+$, TT, and G$^-$T; (2). The absolute configuration of (+)-1,1-dimethyl-2-phenylethylphenyl sulfoxide is (*R*), and of (−)-1,1-dimethyl-2-phenylethylphenyl sulfoxide is (*S*).

Methodology

Experimental

The chiral sulfoxide, **1**, was synthesized and enantiomerically separated on a teicoplanin aglycone column (Chirobiotic TAG) as described by Berthod *et al.*[16] using preparative chromatography. The first eluted enantiomer exhibited a (+)-rotation, and the second eluted enantiomer exhibited a (−)-rotation at 675 nm.

About 6 to 8 mg of each enantiomer have been used for all of the VCD, ECD and OR measurements. Optical rotation as a function of concentration was measured on a Autopol IV polarimeter, using a 1.0 dm cell. Due to the limited sample amount available for **1**, solutions were prepared by successive dilutions from the parent stock solution and concentrations in the range of 0.00465–0.000581 M in CCl_4 solvent were used. The intrinsic rotation, which represents specific rotation at infinite dilution, was extracted from the optical rotations at different concentrations, as described before.[17]

The vibrational absorbance and vibrational circular dichroism spectra were recorded on a commercial Fourier transform VCD spectrometer Chiralir. The sample at a concentration of 0.1355 M in CCl_4 solvent was held in a fixed-pathlength cell with BaF_2 windows and 200 μm spacer. The spectra were recorded with 90 min data collection time at 4 cm^{-1} resolution.

In the absorption spectrum presented (Fig. 4), the solvent absorption was subtracted. Similarly, in the presented VCD spectrum (Fig. 5), the baseline was established by subtracting the spectra of two enantiomers and multiplying by 0.5. The sample of (+)-**1** recovered after VCD measurements was used to record electronic circular dichroism (ECD) spectrum on a Jasco J720 spectrometer. The ECD spectrum was recorded in the 200 to 300 nm region, using 0.1 cm path-length cell. The sample concentration was 0.00465 M in hexane.

Calculations

Geometry optimizations as well as absorption and VCD calculations were undertaken with Gaussian 98 program,[18] while the specific rotation and ECD calculations for isolated molecule were performed using Gaussian 03.[19] The optimizations involving simultaneous rotations around bonds A and D have been performed with ModRedundant option using Gaussian 98. All of the calculations have been based on the density functional

theory (DFT) and have utilized B3LYP functional. The basis sets used in these calculations were 6-31G* and 6-31+G. Additional VCD and ECD calculations were also undertaken with 6-311G(2d,2p) basis set. The theoretical absorption and VCD spectrum were simulated with Lorentzian band shapes and 5 cm^{-1} half-width at half-peak height. Since the *ab initio* predicted band positions are higher than the experimental band positions, the calculated frequencies with 6-31G* basis set were scaled by a factor of 0.9613. The theoretical ECD spectra were simulated from the first 25 singlet → singlet electronic transitions using gaussian band shapes and 20 nm half-width at 1/e of peak height.

References

1 M. Mikolajczyk, J. Drabowicz, P. Kielbasinski, *Chiral Sulfur Reagents: Applications in Asymmetric and Stereoselective Synthesis*, CRC Press: New York, 1997.

2 T. Satoh and Y. Kuramochi, *Tetrahedron Lett.*, 1999, **40**, 8815–8818.

3 S. Nakamura, H. Yasuda, Y. Watanabe and T. Toru., *Tetrahedron Lett.*, 2000, **41**, 4157–4160.

4 S. Nakamura, H. Yasuda, Y. Watanabe and T. Toru, *J. Chem. Soc., Perkin Trans. 1*, 1999, 3403–3404.

5 (*a*) D. A. Cogan, G. Liu, K. Kim, B. J. Backes and J. A. Ellman, *J. Am. Chem. Soc.*, 1998, **120**, 8011–8019; (*b*) T. M. Owens, A. J. Souers and J. A. Ellman, *J. Org. Chem.*, 2003, **68**, 3–10; (*c*) S. A. Blum, R. G. Bergman and J. A. Ellman, *J. Org. Chem.*, 2003, **68**, 150–155.

6 (*a*) T. P. Tang, S. K. Volkman and J. A. Ellman, *J. Org. Chem.*, 2001, **66**, 8772–8778; (*b*) F. Yuste, B. Ortiz, A. Carrasco, M. Peralta, L. Quintero, R. Sanchez-Obregon, F. Walls and J. L. G. Ruano, *Tetrahedron: Asymmetry*, 2000, **11**, 3097–3090.

7 F. Colobert, A. Tito, N. Khiar, D. Denni, M. A. Medina, M. Martin-Lomas, J. L. Ruano and G. Solladie, *J. Org. Chem.*, 1998, **63**, 8919–8921.

8 P. Bravo, M. Crucianelli, A. Farina, S. V. Meille, A. Volonterio and M. Zanda, *Eur. J. Org. Chem.*, 1998, 435–440.

9 (*a*) J. Drabowicz, B. Dudzinski, M. Kolasizyk, M. W. Wieczorek and W. R. Majzner, *Tetrahedron: Asymmetry*, 1998, **9**, 1171–1178; (*b*) J. Drabowicz, B. Dudzinski, M. Mikolajczyk, F. Wang, A. Dehlavi, J. Goring, M. Park, C. Rizzo, P. L. Polavarapu, P. Biscarini, M. W. Wieczorek and W. R. Majzner, *J. Org. Chem.*, 2001, **66**, 1122–1129.

10 (*a*) J. Drabowicz, B. Dudzinski and M. Mikolajczyk, *Tetrahedron: Asymmetry*, 1992, **3**, 1231–1234; (*b*) N. Gautier, N. Noiret, C. Nugier-Chauvin and H. Patin, *Tetrahedron: Asymmetry*, 1997, **8**, 501–505.

11 (*a*) P. L. Polavarapu and J. He, *Anal. Chem.*, 2004, **76**, 61A–67A; (*b*) T. B. Freedman, X. Cao, R. K. Dukor and L. A. Nafie, *Chirality*, 2003, **15**, 743–758.

12 For a recent review, see: P. L. Polavarapu, *Chirality*, 2002, **14**, 768–781; P. L. Polavarapu, *Chirality*, 2003, **15**, 284–285.

13 (*a*) N. Berova, K. Nakanishi, R. W. Woody, *Circular dichroism: Principles and Applications*, Wiley-VCD, New York, 2nd edn., 2000; (*b*) N. Harada and K. Nakanishi, *Circular dichroic spectroscopy:exciton coupling in organic stereochemistry*, University Science Books, Mill Valley, CA 1983.

14 (*a*) J. R. Cheeseman, M. J. Frisch, F. J. Devlin and P. J. Stephens, *Chem. Phys. Lett.*, 1996, **252**, 211; (*b*) P. L. Polavarapu, *Mol. Phys.*, 1997, **91**, 551–554; (*c*) C. Diedrich and S. Grimme, *J. Phys. Chem.*, 2003, **107**, 2524–2539.

15 (*a*) K. Mislow, M. M. Green, P. Laur, J. T. Melillo, T. Simmons and A. L. Ternay, *J. Am. Chem. Soc.*, 1965, **87**, 1958–1976; (*b*) C. Rosini, M. I. Donnoli and S. Superchi, *Chem. Eur. J.*, 2001, **7**, 72–79; (*c*) M. I. Donnoli, E. Giorgio, S. Superchi and C. Rosini, *Org. Biomol. Chem.*, 2003, **1**, 3444–3449; (*d*) A. Aamouch, F. J. Devlin, P. J. Stephens, J. Drabowicz, B. Bujnicki and Marian Mikolajczyk., *Chem. Eur. J.*, 2000, **6**(24); (*e*) F. J. Devlin and P. J. Stephens, *J. Phys. Chem. A*, 2002, **106**, 10510–10524; (*f*) P. J. Stephens, A. Aamouche and F. J. Devlin, *J. Org. Chem.*, 2001, **66**, 3671–3677; (*g*) F. J. Devlin, P. J. Stephens, P. Scafato, S. Superchi and C. Rosini, *Tetrahedron: Asymmetry*, 2001, **12**, 1551–1558; (*h*) F. J. Devlin, P. J. Stephens, P. Scafato, S. Superchi and C. Rosini, *Chirality*, 2002, **14**, 400–406; (*i*) P. J. Stephens, F. J. Devlin, J. R. Cheeseman, M. J. Frisch and C. Rosini, *Org. Lett.*, 2002, **4**, 4595–4598.

16 (*a*) A. Berthod, T. L. Xiao, Y. Liu, W. S. Jenks and D. W. Armstrong, *J. Chromatogr., A*, 2002, **955**, 53–69; (*b*) In ref. 14*a*, the chemical structure of **1** was listed incorrectly in Table 1 with an additional CH_2 group as compound #29; also the (*R*) and (*S*) designations were incorrectly assigned in ref. 14*a* for compound #29 and should be interchanged.

17 P. L. Polavarapu, A. Petrovic and F. Wang, *Chirality.*, 2003, **15**, S143–S149.

18 *Gaussian 98* M. J. Frisch, G. W. Trucks, H. B. Schlegel, G. E. Scuseria, M. A. Robb, J. R. Cheeseman, V. G. Zakrzewski, J. A. Montgomery, Jr., R. Stratmann, J. C. Burant, S. Dapprich, J. M. Millam, A. D. Daniels, K. N. Kudin, M. C. Strain, O. Farkas, J. Tomasi, V. Barone, M. Cossi, R. Cammi, B. Mennucci, C. Pomelli, C. Adamo, S. Clifford, J. Ochterski, G. A. Petersson, P. Y. Ayala, Q. Cui, K. Morokuma, D. K. Malick, A. D. Rabuck, K. Raghavachari, J. B. Foresman, J. Cioslowski, J. V. Ortiz, B. B. Stefanov, G. Liu, A. Liashenko, P. Piskorz, I. Komaromi, R. Gomperts, R. L. Martin, D. J. Fox, T. Keith, M. A. Al-Laham, C. Y. Peng, A. Nanayakkara, C. Gonzalez, M. Challacombe, P. M. W. Gill, B. Johnson, W. Chen, M. W. Wong, J. L. Andres, C. Gonzalez, M. Head-Gordon, E. S. Replogle, J. A. Pople, Gaussian, Inc., PittsburghPA, 1998.

19 *Gaussian 03*, M. J. Frisch, G. W. Trucks, H. B. Schlegel, G. E. Scuseria, M. A. Robb, J. R. Cheeseman, J. A. Montgomery, Jr., T. Vreven, K. N. Kudin, J. C. Burant, J. M. Millam, S. S. Iyengar, J. Tomasi, V. Barone, B. Mennucci, M. Cossi, G. Scalmani, N. Rega, G. A. Petersson, H. Nakatsuji, M. Hada, M. Ehara, K. Toyota, R. Fukuda, J. Hasegawa, M. Ishida, T. Nakajima, Y. Honda, O. Kitao, H. Nakai, M. Klene, X. Li, J. E. Knox, H. P. Hratchian, J. B. Cross, C. Adamo, J. Jaramillo, R. Gomperts, R. E. Stratmann, O. Yazyev, A. J. Austin, R. Cammi, C. Pomelli, J. W. Ochterski, P. Y. Ayala, K. Morokuma, G. A. Voth, P. Salvador, J. J. Dannenberg, V. G. Zakrzewski, S. Dapprich, A. D. Daniels, M. C. Strain, O. Farkas, D. K. Malick, A. D. Rabuck, K. Raghavachari, J. B. Foresman, J. V. Ortiz, Q. Cui, A. G. Baboul, S. Clifford, J. Cioslowski, B. B. Stefanov, G. Liu, A. Liashenko, P. Piskorz, I. Komaromi, R. L. Martin, D. J. Fox, T. Keith, M. A. Al-Laham, C. Y. Peng, A. Nanayakkara, M. Challacombe, P. M. W. Gill, B. Johnson, W. Chen, M. W. Wong, C. Gonzalez, and J. A. Pople, Gaussian, Inc., Wallingford CT, 2004.